

Stiffness Analysis of 3-PRS Parallel Kinematic Mechanism

L. A. Khan¹, M. Rameez², K. Nazir³, H. Liaquat⁴, A. Raza⁵, T.U. Islam⁶

^{1,3,4,5,6} Department of Mechanical Engineering, National University of Technology, Islamabad, Pakistan

² Department of Mechanical Engineering, Capital University of Science and Technology, Islamabad, Pakistan

¹liaquatkhan@nutech.edu.pk

Abstract- Parallel kinematic manipulators have a well advantage over the serial manipulators as a result of their increased stiffness and load carrying capacity. This advantage has increased parallel mechanisms' use in a variety of applications. This article discusses the stiffness analysis of prismatic revolute and spherical (3-PRS) parallel mechanisms in detail. A simple and comprehensive approach is presented to estimate stiffness model of 3-PRS mechanism.

3PRS manipulator has three identical limbs with each limb has prismatic revolute and spherical joint. The proposed 3-PRS mechanism's CAD model is created using Autodesk® inventor professional software. Forward and inverse kinematic model are available. Stiffness models are made analytically as well as the CAD model and analysed using FEA analysis. Analytically and FEA analysis of the CAD model are compared. The results are very close to CAD model, thereby supporting the validity of the presented approach.

Keywords- Kinematics, Prismatic Revolute Spherical, Parallel manipulators, CAD model, Stiffness model

NOMENCLATURE

CNC	Computerized Numerical Control
SPS	Spherical Prismatic Spherical
RRR	Revolute Revolute Revolute
RPS	Revolute Prismatic Spherical
PSP	Prismatic Spherical Prismatic
CAD	Computer Aided Design
FEA	Finite Element Analysis
PKM	Parallel Kinematic Manipulator
PRS	Prismatic Revolute Spherical
PRPR	Prismatic Revolute Prismatic Revolute
PUU	Prismatic Universal Universal
UPU	Universal Prismatic universal

I. INTRODUCTION

Robots play an important role in manufacturing, especially for automation with

improved quality products in industry. Now a day the robots are flexible and can be capable to produce different variety of products. They are faster, accurate and reliable. Robots are preferred due to their low manufacturing cost and accuracy. Robots have many applications in industry like automobile industry that is totally automated production lines or a machine tool manufacturing industry with CNC machines. Other applications include automated production system in pharmaceutical industry, process industry, packing industry and so on. The increase dependence of industrial work on robots is due to its cheaper manufacturing cost, more efficient and accurate work.

Recently, Sun examined the global performance index of the 3-PRS parallel mechanism in terms of linear velocity, acceleration, angular velocity, and angular acceleration using the Jacobean matrix and second order influence coefficient matrix. [1]. Historically, Parallel manipulator firstly introduced by Gough and Whitehall [2] for universal tire testing machine, in which they used 6 universal jacks in parallel arrangement and introduce a new trend in the field of parallel manipulators. Stewart was then introduced the platform for airplane simulator [3]. Kinematic study of parallel manipulator was 1st introduced by Hunt [4]. Different researcher studied parallel mechanism in different ways [5], up to now almost 100 of different kinematic configuration of parallel manipulators are proposed. Parallel manipulators classified in two main branches, planner and spatial manipulator. Planner parallel manipulator has also studied for kinematic position analysis by Gosselin & Angeles [6]. They introduced a 3-RRR (revolute revolute revolute) configuration in planner manipulator. Detail position analysis of planner manipulator is found in [5]. 6-DOF (degree of freedom) spatial parallel manipulator is mostly studied to date which consists of six actuators. Kinematic Analysis of most commonly 6-DOF Stewart Gough mechanism with SPS limb configuration is found in [6].

Tripod based 3DOF parallel manipulator were studied by many researchers for their kinematic performance and workspace volume. A general 3RPS parallel manipulator was studied by Lee and Shah [8], for kinematic analysis. Up to now tripod

parallel manipulators are developed for many configurations like, PRS (prismatic revolute spherical), SPS (spherical, prismatic, spherical), RPS (revolute, prismatic, spherical), etc. Carretero, et al. [9] introduced 3PRS manipulator with each limb have prismatic revolute and spherical arrangements, the inverse position model was derived and addressed the issues with the parasitic motions and optimization of the architecture for parasitic motion minimization. In Carretero et al. model three actuators lies on the same plane with zero inclination angles γ . Tsai, et al. [10] introduce a new architecture design for 3PRS mechanism, in which three actuators are parallel to each other and have the inclination angle γ is equal to 90° . Forward kinematics of that model was solved. A new architecture with the actuator line of action intersect at common point at angle γ , inverse kinematics of this type of manipulator is solved and a square Jacobean is derived by the screw theory, both dexterous and reachable workspace is analysed at different inclination angle [11]. S. Ramana Bab, et.al, formulate a multi-objective optimization problem considering the performance indices are as the objective functions. Three performance criteria-Global conditioning index (GCI), Global stiffness index (GSI) and workspace volume-were formulated and the effect of actuator layout angle on the performance indices was studied. A multi-objective evolutionary algorithm based on the Control elitist non-dominated sorting genetic algorithm (CENSGA) was adopted to find the final approximation set [12]. Antonio Ruiz e. al. made the mechatronic model of a compliant 3PRS parallel manipulator is developed, integrating the inverse and direct kinematics, the inverse dynamic problem of the manipulator and the dynamics of the actuators and its control. The kinematic problem is solved, assuming a pseudo-rigid model for the deflection in the compliant revolute and spherical joints. The inverse dynamic problem is solved, using the Principle of Energy Equivalence [13]. Mervin Joe Thomas made the kinematic and dynamic analysis of a novel 3-PRUS (P: prismatic joint, R: revolute joint, U: universal joint, S: spherical joint) parallel manipulator with a mobile platform having 6 Degree of Freedom (DoF). The kinematic equations for the proposed spatial parallel mechanism were formulated using the Modified Denavit-Hartenberg (DH) technique considering both active and passive joints. A Jacobian based stiffness analysis is done to understand the variations in stiffness for different poses of the mobile platform and further, it is used to decide trajectories for the end effector within the singularity free region [14].

II. MATERIAL AND METHODS

A. Mechanism Description

Fig 1 depicts the 3PRS manipulator's CAD model. The mechanism is composed of a fixed base, a moving platform, and a structure. Three kinematic chains connect the moving platform to the fixed base. Each limb is comprised of a series of Prismatic, Revolute, and Spherical Joints. Three actuators at each link operate the prismatic joint. Three identical prismatic, revolute, and spherical linkages form the total kinematic structure. Three degrees of freedom are available in the 3-PRS mechanism; one is vertical translation and the other two are rotations about two axes in the horizontal plane. The vector representation of the 3-PRS mechanisms are shown in Fig 2. The fixed based triangle $\Delta A_1A_2A_3$ has the center point O at which a Cartesian reference frame $O\{x y z\}$ is attached. Point P is attached to the center of moving platform with the coordinate frame $P\{u v w\}$ and the moving platform triangle $\Delta B_1B_2B_3$. vector OA_1 is in the direction of x -axis and the vector OB_1 is in the direction of u -axis.

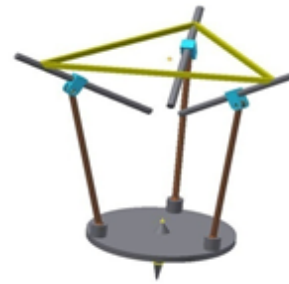


Fig..1 The CAD model of the 3PRS manipulator

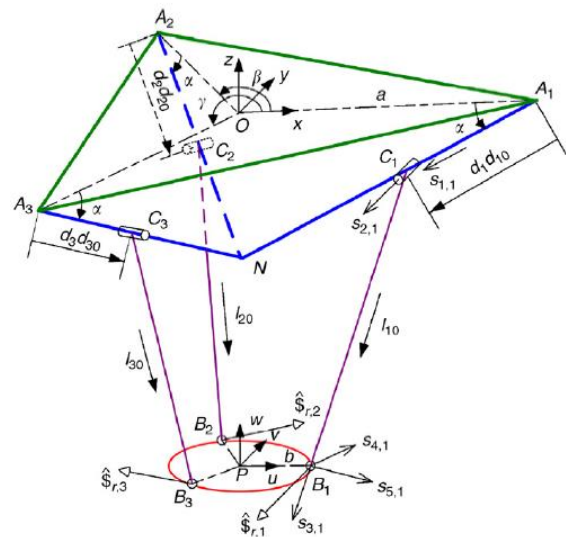


Fig.2 Vector representation of the 3-PRS mechanism

B. Manipulator Geometry

From the geometry of the 3-PRS manipulator three linear actuators for $i = 1$ to 3 A_iN intersect at common point N . Point A_i lies on a circle with radius a . other parameters are listed below.

a is the fixed base platform radius b is the moving platform radius l is the fixed length of each leg α is the actuator layout angle β is the $\angle OA_1$ to OA_2 and $\angle OB_1$ to OB_2

p is the position vector $\{p_x p_y p_z\}^T$ from O to P γ is the $\angle OA_1$ to OA_3 and $\angle OB_1$ to OB_3

φ is the angle between fixed based and fixed leg length $C_i B_i$ q_i is the vector from O to B_i

L_i is the vector from A_i to B_i d is the set of actuated joint variables $=\{d_1 d_2 d_3\}^T$

ϕ, ψ & θ are the Euler Angles X is the set of Cartesian variables $=\{p_x p_y p_z \phi \psi \theta\}^T$

u, v & w are the unit vectors of moving platform x, y & z are the unit vectors of fixed base

The rotation matrix from O to P in terms of direction cosines can be written as

$${}^A R_B = {}^O R_P = \begin{bmatrix} u_x & v_x & w_x \\ u_y & v_y & w_y \\ u_z & v_z & w_z \end{bmatrix} \quad (1)$$

$${}^O R_P = R_y(\theta)R_x(\psi)R_z(\phi) = \begin{bmatrix} c\theta c\phi + s\psi s\theta s\phi & -c\theta s\phi + s\psi s\theta c\phi & c\psi c\theta \\ c\psi s\phi & c\psi c\phi & -s\psi \\ -s\theta c\phi + s\psi c\theta s\phi & s\theta s\phi + s\psi c\theta c\phi & c\psi c\theta \end{bmatrix} \quad (2)$$

Where c represents the cosine and s represents the sine trigonometric functions. The total transformation from the moving platform to the fixed base is composition of rotation matrix ${}^O R_P$ and the position vector $p = \{p_x p_y p_z\}^T$. From the Fig.2 the position vectors from frame O to point A_i and frame P to point B_i can be describe by notation ${}^O a_i$ and ${}^P b_i$, respectively. The leading superscript can be omitted in case of the fixed frame O e.g ${}^O a_i = a_i$. for $i = 1$ to 3 these vectors can be written as.

$$\begin{aligned} a_1 &= [a \ 0 \ 0]^T a_2 = [-a/2 \ \sqrt{3}a/2 \ 0]^T a_3 \\ &= [-a/2 \ -\sqrt{3}a/2 \ 0]^T \\ {}^P b_1 &= [b \ 0 \ 0]^T {}^P b_2 = [b/2 \ -\sqrt{3}b/2 \ 0]^T \\ {}^P b_1 &= [b \ 0 \ 0]^T {}^P b_2 = [b/2 \ -\sqrt{3}b/2 \ 0]^T \\ {}^P b_3 &= [-b/2 \ -\sqrt{3}b/2 \ 0]^T \end{aligned} \quad (3)$$

From Fig.2 the vector loop equation

$$q_i = p + b_i \text{ Where } b_i = {}^O R_P {}^P b_i$$

From Eq-(1) (2) & (3) and by simplifying Eq-(4) is obtained.

$$q_1 = \begin{bmatrix} p_x + b u_x \\ p_y + b u_y \\ p_z + b u_z \end{bmatrix}$$

$$\begin{aligned} q_2 &= \begin{bmatrix} p_x - b u_x/2 + \sqrt{3}b v_x/2 \\ p_y - b u_y/2 + \sqrt{3}b v_y/2 \\ p_z - b u_z/2 + \sqrt{3}b v_z/2 \end{bmatrix} \\ q_3 &= \begin{bmatrix} p_x - b u_x/2 - \sqrt{3}b v_x/2 \\ p_y - b u_y/2 - \sqrt{3}b v_y/2 \\ p_z - b u_z/2 - \sqrt{3}b v_z/2 \end{bmatrix} \end{aligned} \quad (4)$$

The mechanical constraints imposed by the revolute joint in which the spherical joint S can only be move in plane defined by their linear actuator and the fixed leg lengths. Hence

$$\frac{q_{iy}}{q_{ix}} = \tan(*) \quad (5)$$

Where for $i = 1$ to 3 $*$ = $0, \beta$ and γ respectively. From Eq. (5) for $i = 1$ to 3 , we get following three equations.

$$q_{1y} = 0 \quad (6)$$

$$q_{2y} = -\sqrt{3}q_{2x} \quad (7)$$

$$q_{3y} = \sqrt{3}q_{3x} \quad (8)$$

Substituting the elements of q_i from Eq. (4) into Eq. (6), (7) and (8), yields the following equations.

$$p_y + b u_y = 0 \quad (9)$$

$$p_y - b u_y/2 + \sqrt{3}b v_y/2 = -\sqrt{3}(p_x - b u_x/2 + \sqrt{3}b v_x/2) \quad (10)$$

$$p_y - b u_y/2 + \sqrt{3}b v_y/2 = \sqrt{3}(p_x - b u_x/2 + \sqrt{3}b v_x/2) \quad (11)$$

By simplifying Eq.-(9),(10) & (11) we get

$$v_x = u_y \quad (12)$$

After subtracting Eq. (10) from Eq. (11).

$$p_x = \frac{b}{2}(u_x - v_y) \quad (13)$$

Hence, motion of the moving platform is constraints by three equations (9), (12) and (13).

C. Stiffness Analysis

In many applications, the moving platform of a parallel manipulator is in contact with a stiff environment, and applies force to the environment. As the Jacobean transpose is a projection map between the applied force to the environment and the actuator forces causing this moment. The focus is on the deflections of the manipulator's moving platform that are the result of the applied moment to the environment. In parallel manipulators, stiffness is an important performance parameter spatially in high-speed machine tool application for higher accuracy. When the end effector moves to perform a specific task, it exerts some force and/or moment, which cause the end effector deflection form desired location. This deflection is a function of the stiffness and the applied force; thus, the stiffness has a direct effect on the manipulator's positional accuracy. There are many factors that affect the

stiffness e.g. material and size of the manipulator links, actuators and the mechanical transmission system. The most important factor is the structure of the manipulator. Using closed-kinematic chains in the structure of the robot contributes significantly to higher stiffness and better positioning accuracy. The links are assumed to be perfectly rigid in this case. The stiffness of the parallel manipulator can be described by the stiffness matrix. The stiffness matrix represents the relationship between the forces and torques applied to the end effector in Cartesian space and the corresponding Cartesian linear and angular displacements.

Let $\tau = [\tau_1, \tau_2, \dots, \tau_n]^T$ is the vector of actuators joint torque or force and the joint deflection $\Delta q = [\Delta q_1, \Delta q_2, \dots, \Delta q_n]^T$. τ and Δq can be related by $n \times n$ diagonal matrix. Let $\chi = \text{diag}[k_1, k_2 \dots k_n]$ so the relation will become as.

$$\tau = \chi \Delta q \quad (14)$$

The joint deflection Δq is related to end effector deflection Δx by the Jacobean matrix.

$$\Delta q = J \Delta x \quad (15)$$

Where $\Delta x = [\Delta p_x, \Delta p_y, \Delta p_z, \Delta \phi, \Delta \psi, \Delta \theta]^T$

$F = [f, n]^T$ is the vector of output force and moment, which is related to the joint torque τ by jacobian matrix as.

$$F = J^T \tau \quad (16)$$

Putting the Δq from Eq. (15). into Eq.(14) and the resulting equation is

$$F = J^T \chi J \Delta x \quad (17)$$

Here $K = J^T \chi J$ and it is called the stiffness matrix for the parallel manipulator. However, the stiffness matrix is symmetric positive semi-definite, and it depends upon the manipulator configuration. When all the actuators are the same type, the stiffness constant will also be same as $k = k_1 = k_2 = \dots k_n$ then Eq.(17) will be reduced to the form.

$$K = k J^T J. \quad (18)$$

D. Analytical Stiffness Model

The analytical model for the 3 PRS parallel kinematic manipulator is obtained by combining the unit vectors of the fixed base, actuators, fixed leg, and moving platform into the final Jacobean matrix.

$J = J_a \times J_r$ Into final Jacobean matrix $J = J_a J_r$.

$$\text{Where } J_a = J_q^{-1} J_x \text{ and } J_r = \begin{bmatrix} \frac{\partial P_x}{\partial P_z} & \frac{\partial P_x}{\partial \psi} & \frac{\partial P_x}{\partial \theta} \\ \frac{\partial P_y}{\partial P_z} & \frac{\partial P_y}{\partial \psi} & \frac{\partial P_y}{\partial \theta} \\ 1 & 0 & 0 \\ 0 & 1 & 0 \\ 0 & 0 & 1 \\ \frac{\partial P_\phi}{\partial P_z} & \frac{\partial P_\phi}{\partial \psi} & \frac{\partial P_\phi}{\partial \theta} \end{bmatrix} \quad (19)$$

To find the Jacobean matrix J_a we need to put unit

$$\text{vector of } J_x \text{ \& } J_q \quad J_x = \begin{bmatrix} I_{10} & (b_1 \times I_{10})^T \\ I_{20} & (b_2 \times I_{20})^T \\ I_{30} & (b_3 \times I_{30})^T \end{bmatrix}_{3 \times 6} \quad (20)$$

$$I_{i0} = \frac{L_i - d_i d_{i0}}{l} \quad (20)$$

$$L_i = q_i - a_i \quad (21)$$

$$q_1 = \begin{bmatrix} \frac{3}{2} b u_x - b v_y \\ 0 \\ p_z + b u_z \end{bmatrix}$$

$$q_2 = \begin{bmatrix} -b v_y/2 + \sqrt{3} b v_x/2 \\ -3 b u_y/2 + \sqrt{3} b v_y/2 \\ p_z - b u_z/2 + \sqrt{3} b v_z/2 \end{bmatrix}$$

$$q_3 = \begin{bmatrix} -b v_y/2 - \sqrt{3} b v_x/2 \\ -3 b u_y/2 - \sqrt{3} b v_y/2 \\ p_z - b u_z/2 - \sqrt{3} b v_z/2 \end{bmatrix} \quad (22)$$

Values of L_i are found using Eq.(21)

$$L_1 = \begin{bmatrix} \frac{3}{2} b u_x - b v_y - a \\ 0 \\ p_z + b u_z \end{bmatrix}$$

$$L_2 = \begin{bmatrix} -b v_y/2 + \sqrt{3} b v_x/2 + a/2 \\ -3 b u_y/2 + \sqrt{3} b v_y/2 - \sqrt{3} a/2 \\ p_z - b u_z/2 + \sqrt{3} b v_z/2 \end{bmatrix}$$

$$L_3 = \begin{bmatrix} -b v_y/2 - \sqrt{3} b v_x/2 + a/2 \\ -3 b u_y/2 - \sqrt{3} b v_y/2 + \sqrt{3} a/2 \\ p_z - b u_z/2 - \sqrt{3} b v_z/2 \end{bmatrix} \quad (23)$$

Unit vector I_{i0} can be obtained from Eq.(20)

$$I_{i0} = \frac{L_i - d_i d_{i0}}{l}$$

$$I_{10} = \begin{bmatrix} \frac{2d_1 c a + 3 b u_x - b v_y - 2a}{2l} \\ 0 \\ \frac{d_1 s a + p_z + b u_z}{l} \end{bmatrix} \quad (24)$$

$$I_{20} = \begin{bmatrix} \frac{-d_2 c a + \sqrt{3} b v_x - b v_y + a}{2l} \\ \frac{d_2 \sqrt{3} c a - 3 b u_y + \sqrt{3} b v_y - \sqrt{3} a}{2l} \\ \frac{2d_2 s a + 2p_z - b u_z + \sqrt{3} b v_z}{2l} \end{bmatrix} \quad (25)$$

$$I_{30} = \begin{bmatrix} \frac{-d_3 c a - \sqrt{3} b v_x - b v_y + a}{2l} \\ \frac{-d_3 \sqrt{3} c a - 3 b u_y - \sqrt{3} b v_y + \sqrt{3} a}{2l} \\ \frac{2d_3 s a + 2p_z - b u_z - \sqrt{3} b v_z}{2l} \end{bmatrix} \quad (26)$$

From section of analytical model the Jacobean can be found

$$J_x = \begin{bmatrix} I_{10} & (b_1 \times I_{10})^T \\ I_{20} & (b_2 \times I_{20})^T \\ I_{30} & (b_3 \times I_{30})^T \end{bmatrix}_{3 \times 6}$$

The unit vectors are

$$b_1 = \begin{bmatrix} bu_x \\ bu_y \\ bu_z \end{bmatrix}$$

$$b_2 = \begin{bmatrix} -bu_x/2 + \sqrt{3}bv_x/2 \\ -bu_y/2 + \sqrt{3}bv_y/2 \\ -bu_z/2 + \sqrt{3}bv_z/2 \end{bmatrix}$$

$$b_3 = \begin{bmatrix} -bu_x/2 - \sqrt{3}bv_x/2 \\ -bu_y/2 - \sqrt{3}bv_y/2 \\ -bu_z/2 - \sqrt{3}bv_z/2 \end{bmatrix} \quad (27)$$

Taking cross product of b_1, b_2 and b_3 of Eq.(26) with Eq. (24), (25) and (26).

Finally, a 3 x 6 Jacobean matrix is obtained.

$$J_a = \begin{bmatrix} a_{11} & a_{12} & a_{13} & a_{14} & a_{15} & a_{16} \\ a_{21} & a_{22} & a_{23} & a_{24} & a_{25} & a_{26} \\ a_{31} & a_{32} & a_{33} & a_{34} & a_{35} & a_{36} \end{bmatrix} \quad (28)$$

Where,

$$a_{11} = -\frac{2d_1ca+3bu_x-bv_y-2a}{2d_1+2sab u_z+3cab u_x-ca b v_y+2sap_z-2aca}$$

$$a_{12} = 0$$

$$a_{13} = -\frac{2(d_1sa+b u_z+p_z)}{2d_1+2sab u_z+3cab u_x-ca b v_y+2sap_z-2aca}$$

$$a_{14} = -\frac{2b u_y(d_1sa+b u_z+p_z)}{2d_1+2sab u_z+3cab u_x-ca b v_y+2sap_z-2aca}$$

$$a_{15} = \frac{b(2sa d_1u_x-2ca d_1u_z-bu_xu_z+bu_zv_y+2a u_z+2p_zu_x)}{2d_1+2sab u_z+3cab u_x-ca b v_y+2sap_z-2aca}$$

$$a_{16} = \frac{b u_y(2d_1ca+3bu_x-bv_y-2a)}{2d_1+2sab u_z+3cab u_x-ca b v_y+2sap_z-2aca}$$

$$a_{21} = \frac{2(-\sqrt{3}b v_x+d_2ca+b v_y-a)}{4d_2+4cab v_y-4a ca-3ca \sqrt{3}b buy-ca \sqrt{3}b v_x+2sa \sqrt{3}b v_z-2sa b u_z+4sa p_z}$$

$$a_{22} = \frac{2(d_2\sqrt{3}ca+\sqrt{3}b v_y-\sqrt{3}a-3b u_y)}{4d_2+4cab v_y-4a ca-3ca \sqrt{3}b buy-ca \sqrt{3}b v_x+2sa \sqrt{3}b v_z-2sa b u_z+4sa p_z}$$

$$a_{23} = \frac{2(\sqrt{3}b v_z+2d_2sa-bu_z+2p_z)}{4d_2+4cab v_y-4a ca-3ca \sqrt{3}b buy-ca \sqrt{3}b v_x+2sa \sqrt{3}b v_z-2sa b u_z+4sa p_z}$$

$$a_{24} = -\frac{x_1 + x_2}{y_1 + y_2}$$

$$x_1 = b(2sa\sqrt{3}d_2v_y + 2\sqrt{3}b u_yv_z - 2sad_2u_y + 2\sqrt{3}p_zv_y - 2bu_yu_z)$$

$$x_2 = 2p_zu_y - 3cad_2v_z + ca\sqrt{3}d_2u_z + 3a v_z - \sqrt{3}a u_z$$

$$y_1 = 4d_2 + 4cab v_y - 4a ca - 3ca \sqrt{3}b buy$$

$$y_2 = ca \sqrt{3}b v_x + 2sa \sqrt{3}b v_z - 2sa b u_z + 4sa p_z$$

$$a_{25} = \frac{b(x_3 + x_4)}{y_1 + y_2}$$

$$x_3 = 2sa\sqrt{3}d_2v_x - \sqrt{3}bu_xv_z - 2sad_2u_x + 2\sqrt{3}p_zv_x + bu_xu_z - 2p_zu_x$$

$$x_4 = ca\sqrt{3}d_2v_z + \sqrt{3}bv_yv_z - cad_2u_z - \sqrt{3}av_z - bu_zv_y + au_z$$

$$a_{26} = \frac{b(x_5 - x_6)}{y_1 + y_2}$$

$$x_5 = ca\sqrt{3}d_2u_x - ca\sqrt{3}d_2v_y + \sqrt{3}bu_xv_y + 2\sqrt{3}bu_yv_x - \sqrt{3}bv_y^2 + cad_2u_y$$

$$x_6 = 3cad_2v_x - \sqrt{3}au_x + \sqrt{3}av_y - 3bu_xu_y + bu_yv_y - au_y + 3av_x$$

$$a_{31} = \frac{x_7}{y_1 + y_2}$$

$$x_7 = 2(\sqrt{3}bv_x + d_3ca + bv_y - a)$$

$$a_{32} = \frac{x_8}{y_1 + y_2}$$

$$x_8 = 2(d_3\sqrt{3}ca + \sqrt{3}b v_y - \sqrt{3}a + 3b u_y)$$

$$a_{33} = \frac{x_9}{y_1 + y_2}$$

$$x_9 = 2(2d_3sa - \sqrt{3}bv_z - bu_z + 2p_z)$$

$$a_{34} = \frac{-b(x_{10} + x_{11})}{y_1 + y_2}$$

$$x_{10} = 2sa\sqrt{3}d_3v_y + 2\sqrt{3}bu_yv_z + 2sad_3u_y + 2\sqrt{3}p_zv_y + 2bu_yu_z$$

$$x_{11} = 2p_zu_y + 3cad_3v_z + ca\sqrt{3}d_3u_z - 3av_z - \sqrt{3}au_z$$

$$a_{35} = \frac{b(x_{12} + x_{13})}{y_1 + y_2}$$

$$x_{12} = 2sa\sqrt{3}d_3v_x - \sqrt{3}bu_xv_z + 2sad_3u_x + 2\sqrt{3}p_zv_x - bu_xu_z + 2p_zu_x$$

$$x_{13} = ca\sqrt{3}d_3v_z + \sqrt{3}bv_yv_z + ca\sqrt{3}d_3u_z - \sqrt{3}av_z + bu_zv_y - au_z$$

$$a_{36} = \frac{-b(x_{14} + x_{15})}{y_1 + y_2}$$

$$x_{14} = 3cad_3v_x + ca\sqrt{3}d_3u_x - ca\sqrt{3}d_3v_y - 3av_x + \sqrt{3}bu_xv_y + 2\sqrt{3}bu_yv_x$$

$$x_{15} = \sqrt{3}bv_y^2 - cad_3u_y - \sqrt{3}au_x + \sqrt{3}av_y + 3vu_xu_y - bu_yv_y + au_y$$

To find J_r the derivative from the constraints are

$$J_r = \begin{bmatrix} \frac{\partial P_x}{\partial P_z} & \frac{\partial P_x}{\partial \psi} & \frac{\partial P_x}{\partial \theta} \\ \frac{\partial P_y}{\partial P_z} & \frac{\partial P_y}{\partial \psi} & \frac{\partial P_y}{\partial \theta} \\ \frac{\partial P_\phi}{\partial P_z} & \frac{\partial P_\phi}{\partial \psi} & \frac{\partial P_\phi}{\partial \theta} \end{bmatrix}_{6 \times 3} \quad (29)$$

$$\frac{\partial P_x}{\partial P_z} = 0$$

$$\frac{\partial P_x}{\partial \psi} = -\frac{(s\psi b(c\theta^3 c\psi^2 + 2c\theta^2 c\psi - 2c\theta c\psi^2 - c\theta - 4c\psi))}{2(c\psi c\theta + 1)^2}$$

$$\frac{\partial P_x}{\partial \theta} = -\frac{c\psi s\theta b(c\psi^2 c\theta^2 + 2c\psi c\theta - 2c\psi^2 - 1)}{2(c\psi c\theta + 1)^2}$$

$$\frac{\partial P_y}{\partial P_z} = 0$$

$$\frac{\partial P_y}{\partial \psi} = \frac{-bs\theta(c\psi^3 c\theta + 2c\psi^2 - 1)}{(c\psi c\theta + 1)^2}$$

$$\frac{\partial P_y}{\partial \theta} = \frac{-bc\psi(c\psi + c\theta s\psi)}{(c\psi c\theta + 1)^2}$$

$$\frac{\partial P_\phi}{\partial P_z} = 0$$

$$\frac{\partial P_\phi}{\partial \psi} = \frac{s\theta}{c\psi c\theta + 1}$$

$$\frac{\partial P_\phi}{\partial \theta} = \frac{s\psi}{c\psi c\theta + 1}$$

Finally, the Jacobean matrix is

$$J = J_a J_r = \begin{bmatrix} j_{11} & j_{12} & j_{13} \\ j_{21} & j_{22} & j_{23} \\ j_{31} & j_{32} & j_{33} \end{bmatrix}_{3 \times 3} \quad (30)$$

III. RESULTS AND DISCUSSION

The parameters used for the stiffness model is listed in Table-1

Table -1 Architecture Parameters For 3 Prs Manipulator

Parameters	
a	400mm
b	200mm
l	550mm
α	30°

Stiffness Analysis Results

The architecture parameters for 3PRS manipulator is given in table-1 and stiffness constant is taken to be 19500 N/mm for each of the linear actuator. A MATLAB program written to determine the stiffness of the general 3PRS mechanism at its maximum and minimum values. The results are shown in Fig 4 and in Fig.5. Let $p_z = -0.59$ M from configuration -1 and corresponding values for ψ & θ are -0.751 and -0.089 respectively. The results show the value of maximum stiffness at this point, is equal to be 156.448 kN/m.

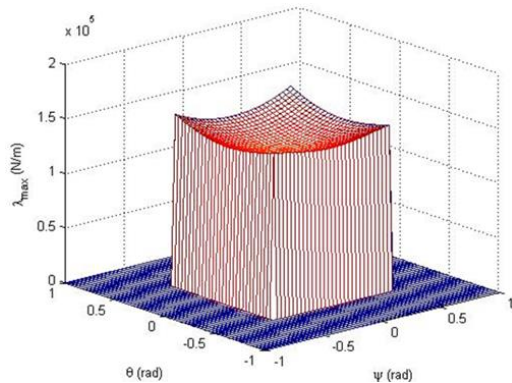


Fig.3 Maximum stiffness of 3PRS mechanism at height $P_z = -0.59$ m

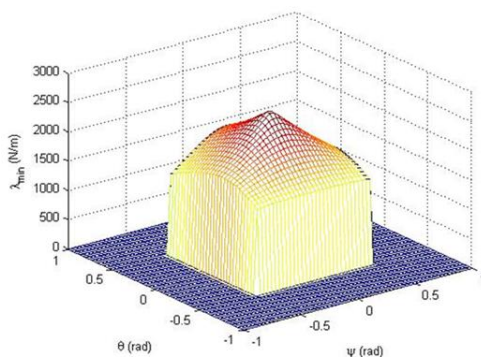
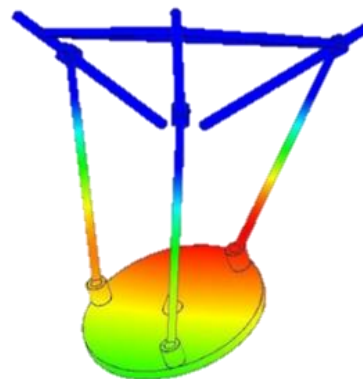
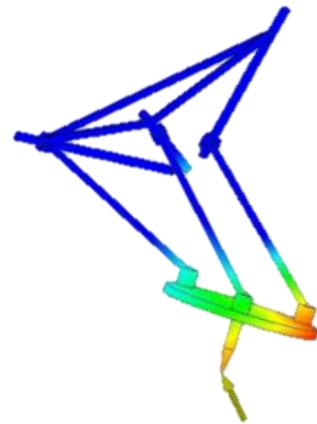
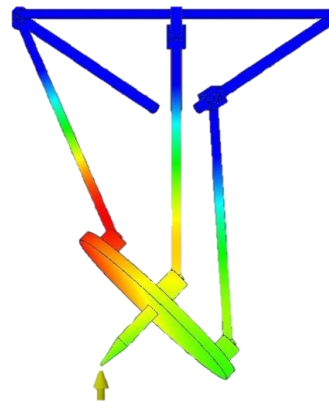


Fig 4 Minimum stiffness of 3PRS mechanism at height $P_z = -0.59$ m

The detail design of the 3PRS is carried out on CAD software AUTODESK INVENTOR PROFESSIONAL® with the same parameters as described in table 1. the stiffness of the model is also carried out on stress analysis tool for configuration-1 as shown in fig 9 with 0.1 KN force is applied at the tool tip. Fig 8 shows the total displacement of the manipulator. The stiffness can be obtained by the relation $(F)/\Delta x$. Where F denotes the applied force and Δx is the total deflection. From the model FEA analysis we obtain the maximum stiffness = 156.274 kN/m. Table 2 shows the comparison of results with both numerical model and the FEA model. Fig 5 is showing the displacement distribution along X-axis, Y-axis and Z-axis respectively.



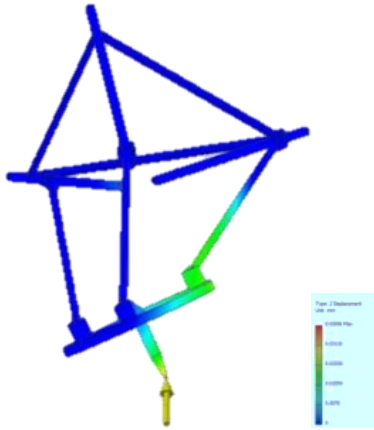


Fig 5 Total deformation, deformation in X-axis, Y-axis and Z-axis showing in figures in sequence these are represented.

The comparison of stiffness results using numerical model is having only an error of 0.1%, which is very small and hence the stiffness analysis of 3PRS mechanism is done and verified.

Table 2: Comparison of Results Obtain from Numerical Method and Fea Model

Maximum Stiffness (kN/m)	
Numerical Model	156.448
FEA Model	156.274

IV. CONCLUSIONS

The stiffness analysis of 3PRS manipulator is performed in this paper. The stiffness characteristics of the actuator, as well as the changes in actuator angle (α), are also calculated numerically. The stiffness matrix's minimum and maximum eigenvalues are frequently used as performance indices. These values can be used to estimate the stiffness of 3 PRS manipulator. FEA analysis is performed and results are compared using both analytical and numerical analysis. Both techniques gave a good match as presented by the data in this paper. The difference is only 0.1% in analytical and numerical model.

REFERENCES

[1] Fuwei Sun, Junwei Zhao, Guoqiang Chen, Analysis on Kinematic Performance Index of 3-PRS Parallel Mechanism, *Advanced*

Science and Technology Letters, Vol.143 (AST 2017), pp.106-112

[2] Gough, V. and S. Whitehall. Universal tyre test machine in Proc. FISITA 9th Int. Technical Congress. 1962.

[3] Stewart, D., A platform with six degrees of freedom. *Proceedings of the institution of mechanical engineers*, 1965. 180(1): p. 371-386.

[4] Hunt, K., Structural kinematics of in-parallel-actuated robot-arms. *Journal of Mechanisms, Transmissions, and Automation in Design*, 1983. 105(4): p. 705-712.

[5] Tsai, L.-W., *Robot analysis: the mechanics of serial and parallel manipulators*. 1999: John Wiley & Sons.

[6] Gosselin, C. and J. Angeles, The optimum kinematic design of a planar three-degree-of-freedom parallel manipulator. *Journal of Mechanisms, Transmissions, and Automation in Design*, 1988. 110(1): p. 35-41.

[7] Taghirad, H.D., *Parallel robots: mechanics and control*. 2013: CRC press.

[8] Lee, K.-M. and D.K. Shah, Kinematic analysis of a three-degrees-of-freedom in-parallel actuated manipulator. *IEEE Journal on Robotics and Automation*, 1988. 4(3): p. 354-360.

[9] Carretero, J., et al., Kinematic analysis and optimization of a new three degree-of-freedom spatial parallel manipulator. *Journal of mechanical design*, 2000. 122(1): p. 17-24.

[10] Tsai, M.-S., et al., Direct kinematic analysis of a 3-PRS parallel mechanism. *Mechanism and Machine Theory*, 2003. 38(1): p. 71-83.

[11] Pond, G.T. and J.A. Carretero. Kinematic analysis and workspace determination of the inclined PRS parallel manipulator. in Proc. of 15th CISM-IFTOMM Symposium on Robot Design, Dynamics, and Control. 2004.

[12] S. Ramana Babu et.al, Design optimization of 3PRS parallel manipulator using global performance indices, *Journal of Mechanical Science and Technology*, 30 (9), 2016.

[13] Antonio Ruiz, et.al, *Mechatronic Model of a Compliant 3PRS Parallel Manipulator*, Robotics, MDPI, robotics11010004, 2022.

[14] Mervin Joe Thomas, et.al, Kinematic and Dynamic Analysis of a 3-PRUS Spatial Parallel Manipulator, *Chinese Journal of Mechanical Engineering*, 33:13, 2020.